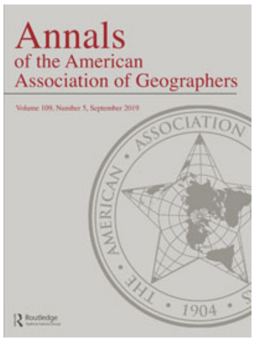

Annals of the American Association of Geographers

ISSN: 2469-4452 (Print) 2469-4460 (Online) Journal homepage: https://www.tandfonline.com/loi/raag21

Urban Geocryology: Mapping Urban–Rural Contrasts in Active-Layer Thickness, Barrow Peninsula, Northern Alaska

Anna E. Klene & Frederick E. Nelson

Urban Geocryology: Mapping Urban–Rural Contrasts in Active-Layer Thickness, Barrow Peninsula, Northern Alaska

Anna E. Klene* and Frederick E. Nelson†

*Department of Geography, University of Montana
†Department of Geography, Environment, and Spatial Sciences, Michigan State University, and Department of Earth, Environmental, and Geographical Sciences, Northern Michigan University

The maximum depth of seasonal thaw is a critical design factor for civil infrastructure in permafrost regions. Although maps of active-layer thickness (ALT) have been created for localized areas in undisturbed terrain, this has rarely been done within urbanized areas. The modified Berggren solution was used to map ALT at a resolution of 30×30 m over the 150-km^2 Barrow Peninsula in northern Alaska. Emphasis was placed on analyzing differences in accuracy obtained in urbanized and relatively undisturbed tundra. Although the modified Berggren solution is known to provide more accurate estimates of frost and thaw depth than the Stefan solution, it has not been used previously in mapping applications. As part of the Barrow Urban Heat Island Study, seventy-one miniature data loggers were installed in and surrounding the City of Utqiaġvik (formerly Barrow) to measure air and soil temperature. The resulting data were used to calculate air and soil surface temperature fields, as well as summer *n*-factors, based on nine urban and rural land-cover classes. Regional soil and land-cover maps were used to obtain additional input data. Validation was performed by comparing probed ALT measurements with predicted pixel values. Model results confirm that the presence of urban infrastructure increases both the magnitude and the geographic variability of ALT relative to surrounding undisturbed tundra. The Berggren solution performed well for estimating mean values for land-cover classes in both rural and urban areas and has considerable potential as a tool for mapping ALT in other applications. *Key Words: active layer, Alaska, Barrow, frozen ground, geocryology, mapping, permafrost, urban, Utqiaġvik.*

解冻季节的最大深度，是在永久冻原地区进行民用基础建设的关键设计因素。尽管未受干扰地域中的在地区域已绘製了活动层厚度（ALT）地图，但在城市化的地区却鲜少有该地图的绘製。本研究运用改良的贝里格伦解决方案，在阿拉斯加北部的一百五十平方公里的巴罗半岛中，以三十平方米的分辨率来绘製ALT。本研究强调分析在城市化与相对较不受干扰的冻原所取得的准确度差异。尽管改良的贝里格伦解决方案被认为能够较斯特凡解决方案更为精确地评估冻和融冻，但该方案过去却未曾应用于製图。作为巴罗城市热岛研究的一部分，七十一个微型数据记录器被安装在乌特洽维克（以前的巴罗）市内与周遭，以测量空气和土壤温度。根据九大城市与乡村土地覆盖分类，研究结果之数据，用来计算空气与土壤表层的温度范畴，以及夏季的n要素。区域土壤和土地覆盖地图用来取得额外的输入数据。该研究并透过比较提出的ALT测量与预估的像素值来进行验证。模型结果确认了城市基础建设的出现， 增加了相较于周遭未受影响的冻原的ALT程度与地理变化性。贝里格伦解决方案在评估乡村与城市地区的土地覆盖分类时皆表现良好，并在作为其他应用绘製ALT的工具上具有庞大的潜能。 *关键词: 活动层, 阿拉斯加, 巴罗, 冻原, 冻土学, 製图, 永久冻土, 城市, 乌特恰维克。*

La profundidad máxima del deshielo estacional es un factor crítico del diseño de infraestructura civil en regiones de permagel. Aunque se han elaborado mapas del espesor de la capa activa (ALT) en áreas específicas de terrenos inalterados, tal cosa rara vez se ha intentado dentro de áreas urbanizadas. La solución Berggren modificada se usó para mapear la ALT a una resolución de 30 x 30m sobre la Península Barrow de 150 km2 en el norte de Alaska. Se hizo énfasis en el análisis de las diferencias en exactitud obtenidas en la tundra urbanizada y en la relativamente inalterada. Aunque se sabe que la solución Berggren modificada genera cálculos más exactos sobre la profundidad del congelamiento y el deshielo que la solución Stefan, no ha sido usada anteriormente en aplicaciones cartográficas. Como parte del Estudio de la Isla de Calor Urbana de Barrow, se instalaron setenta y un registradores de datos en miniatura dentro y en los alrededores de la ciudad de Utqiagvik (antes Barrow) para medir la temperatura del aire y del suelo. Los datos obtenidos

Annals of the American Association of Geographers, 109(5) 2019, pp. 1394–1414 © 2019 by American Association of Geographers
Initial submission, March 2018; revised submission, June 2018; final acceptance, September 2018
Color versions of one or more figures in the article can be found online at www.tandfonline.com/raag
Published by Taylor & Francis, LLC.

se usaron para calcular los campos de la temperatura del aire y de la superficie del suelo, lo mismo que los n-factores de verano, basados en nueve clases de cubiertas del suelo urbanas y rurales. Se usaron mapas regionales del suelo y de la cobertura de la tierra para obtener datos cargados adicionales. La validación se llevó a cabo comparando mediciones de la ALT probadas con valores pixel pronosticados. Los resultados del modelo confirman que la presencia de infraestructura urbana incrementa tanto la magnitud como la variabilidad geográfica de la ALT con relación a la tundra inalterada de los alrededores. La solución Berggren se desempeñó bien en el proceso de calcular los valores medios de las clases de coberturas de la tierra en áreas rurales y urbanas, y tiene un considerable potencial como herramienta para mapear la ALT en otras aplicaciones. *Palabras clave: Alaska, Barrow, capa activa, geocriología, mapeo, permagel, urbano, Utqiagvik.*

As economic and resource development intensify in the world's cold regions, perennially frozen ground has become an increasingly important consideration for Arctic communities. Understanding the dynamics of frozen ground and the ability to predict the behavior of the near-surface seasonally thawed layer is crucial for planning, engineering, construction, and maintenance of infrastructure. Increases in the depth of thaw at locations with ice-rich substrate can lead to differential ground subsidence, creating the potential for structural failure and other problems (e.g., Grebenets 2003; Streletskiy, Shiklomanov, and Nelson 2012; Shiklomanov, Streletskiy, Grebenets, et al. 2017; Shiklomanov, Streletskiy, Swales, et al. 2017). The geographic variability of parameters contributing to the depth of seasonal thaw is very high in natural landscapes but potentially even more so in urban environments, where variations in material properties associated with the built environment are abrupt. Although the vulnerability of infrastructure to thaw-related problems has long been known in Alaska and across the Arctic (e.g., S. W. Muller 1943; Péwé 1966), problematic development practices have continued in some instances.

Permafrost is defined as "ground that remains continuously at or below 0 °C for at least two consecutive years" (van Everdingen 1994, 222). The layer of ground above permafrost that freezes and thaws on an annual basis is known as the *active layer*. Permafrost characteristics are often mapped at small geographical scales (i.e., over very large areas) and at coarse resolution (e.g., Nelson 1986; Shur and Slavin-Borovskiy 1993; Anisimov, Shiklomanov, and Nelson 1997; Brown et al. 1997; Henry and Smith 2001; Burn and Nelson 2006). Although large-scale (local) maps of active-layer thickness (ALT) have been created for small (e.g., 1 ha or 1 km^2) areas of relatively undisturbed terrain (e.g., Nelson et al. 1997; Nelson et al. 1998; Hinkel and Nelson 2003; Mazhitova et al. 2004; Vieira et al. 2010), this has rarely been done within urbanized areas, even though the depth of seasonal thaw is a critical factor in the design of roads, buildings, pipelines, and other infrastructure. The need for detailed maps of ALT is emphasized in work on potential hazards in permafrost regions associated with global warming scenarios (Nelson, Anisimov, and Shiklomanov 2001, 2002; U.S. Arctic Research Commission Permafrost Task Force 2003; Anisimov et al. 2007; Daanen et al. 2011; Romanovsky 2011; Hong, Perkins, and Trainor 2014; Hjort et al. 2018).

Alaska's North Slope is part of a region considered to be at moderate to high risk for thaw-induced damage under sustained climatic warming (U.S. Arctic Research Commission Permafrost Task Force 2003; Hong, Perkins, and Trainor 2014; Olefeldt et al. 2016). Documentation of a winter urban heat island in Barrow (Hinkel, Nelson, et al. 2003; Klene, Hinkel, and Nelson 2003; Hinkel and Nelson 2007), earlier snowmelt in the city than in the surrounding tundra (Stone et al. 2002), and the amount of dust downwind of roads and construction pads (Bodhaine, Harris, and Herbert 1981; Walker and Everett 1987; Raynolds et al. 2014) are all consequences of urban disturbances and can increase ALT. Klene, Nelson, and Hinkel (2013) documented a 17- to 41-cm difference in the depth of thaw between locations in the city and the surrounding undeveloped tundra, even within similar land-cover classes.

Geocryology, the study of frozen rocks, soil, and ground, is often divided into two closely related parts: general geocryology (Yershov 1998) and engineering geocryology (Dement'ev et al. 1959). Here, we introduce the hybrid term *urban geocryology* in recognition of the special problems and high variability of the distribution of frozen ground processes associated with composite, geographically extensive built environments (e.g., Shiklomanov, Streletskiy,

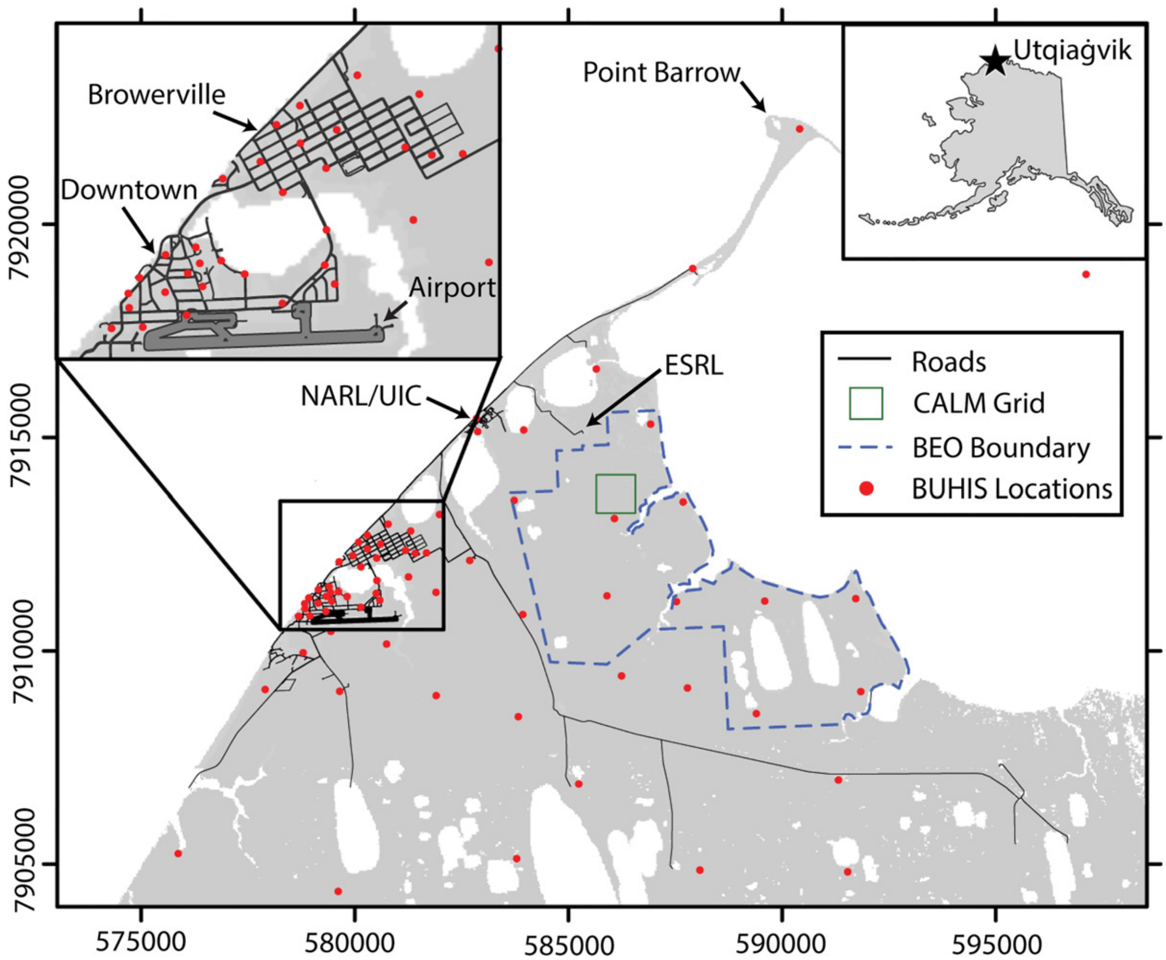

Figure 1. Map of study area. Location of Utqiaġvik (Barrow) is denoted by a black star on the inset map of Alaska. Dots denote BUHIS site locations. Roads are shown as solid lines and the BEO boundary as a dashed line. The airport is at the southern edge of the city. Solid square line within the BEO indicates location of the 1 × 1 km Barrow (U1) CALM grid used for monitoring active-layer thickness. Units along map borders are coordinates in WGS 84, UTM Zone 4N. *Note:* NARL/UIC = Naval Arctic Research Laboratory/Ukpeaġvik Iñupiat Corporation; CALM = Circumpolar Active Layer Monitoring; BEO = Barrow Environmental Observatory; BUHIS = Barrow Urban Heat Island Study.

Grebenets, et al. 2017). The specific focus is mapping ALT in the Barrow Peninsula of northern Alaska, with particular attention given to contrasts between the intensively urbanized City of Utqiaġvik (formerly Barrow; Hersher 2016)[1] and the relatively undisturbed tundra of the nearby Barrow Environmental Observatory (NEON 2018). The modified Berggren solution, an advanced analytic solution to the general Stefan problem of calculating frost and thaw depth (Berggren 1943; Aldrich and Paynter 1966; Zarling, Braley, and Pelz 1989), is used in a geographic context to calculate and map ALT over the 150-km^2 area investigated in the Barrow Urban Heat Island Study (BUHIS) in northern Alaska (Hinkel, Nelson, et al. 2003; Hinkel and Nelson 2007; Klene, Nelson, and Hinkel 2013).

Study Area

The City of Utqiaġvik (71°17′44″N; 156°45′59″W) is the economic, transportation, and administrative hub of Alaska's North Slope Borough, the northernmost community in the United States, and the largest native settlement in the circum-Arctic region. It lies approximately 200 km north of the Brooks Range, with a 100-km-wide area of low-relief terrain between its coastal location and the Arctic Foothills (Figure 1).

Utqiaġvik's location has been used for at least 1,500 years by Iñupiat Eskimos, who constitute about 61 percent of the city's current population of nearly 4,500 residents (U.S. Census Bureau 2018; Utqiaġvik 2018). The area has a long and

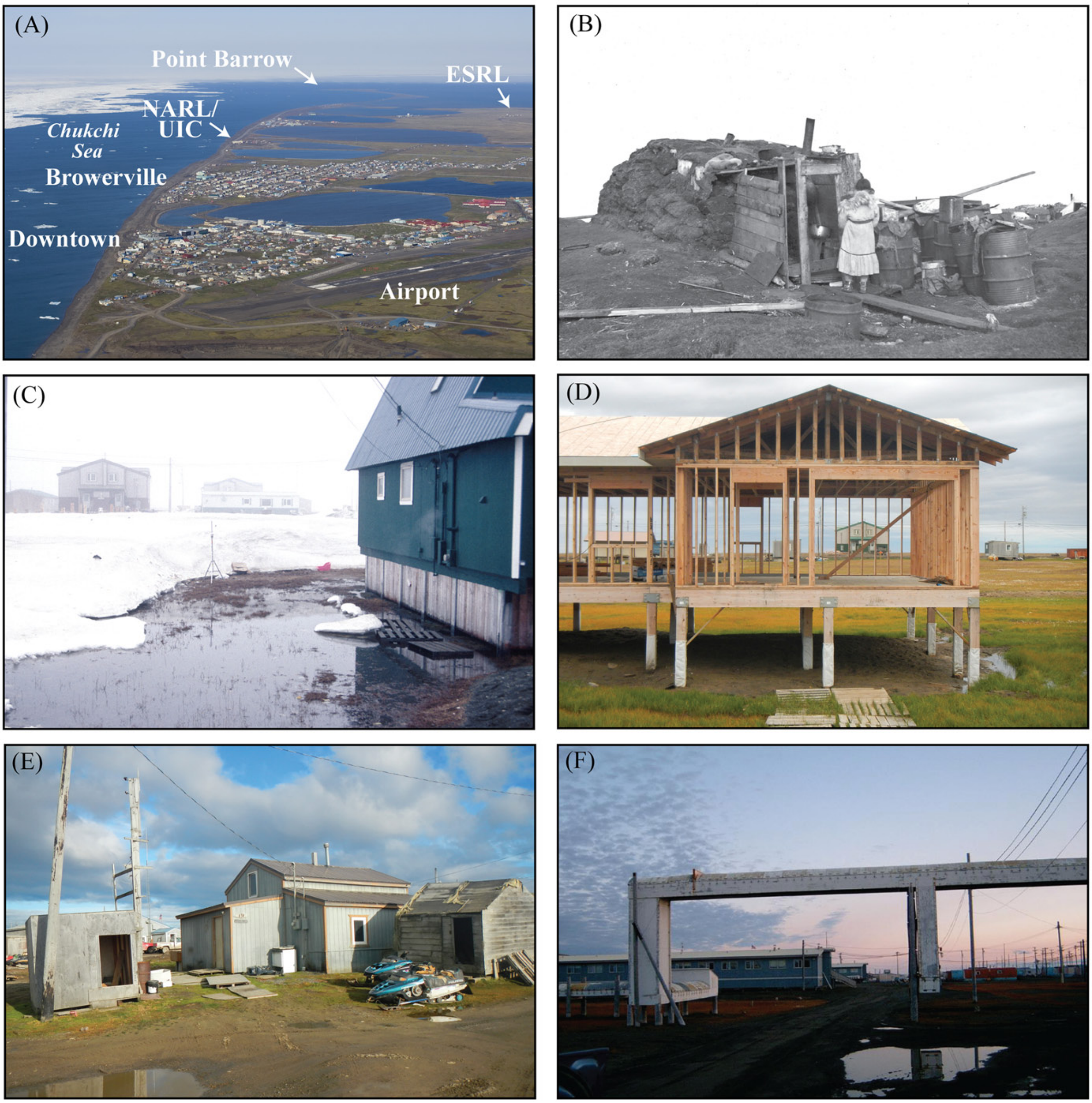

Figure 2. (A) Oblique air photo of the City of Utqiaġvik (Barrow), view to the northeast. Differences in the urban morphology are visible between older downtown and the grid pattern of development in Browerville. Locations referred to in the text are labeled. Photo by Steven Kazlowski, 2006. (B) Traditional sod hut in Barrow. Most such houses were replaced by the mid-twentieth century (Brower 1948). Photo by R. F. Black, 1945, courtesy of U.S. Geological Survey. (C) Yard of house in eastern Browerville during snowmelt. Barrow Urban Heat Island Study monitoring tripod is visible. Ponded water trapped by road network must be pumped out each spring to prevent degradation of underlying permafrost. Photo by Anna E. Klene. (D) New development in eastern Browerville with elevated houses and sand and gravel roads in a grid pattern. Photo by Nikolay Shiklomanov. (E) House near downtown Barrow built with little insulation of the underlying permafrost. Photo by Anna E. Klene. (F) "Utilidor" constructed for NARL, now operated by Ukpeaġvik Iñupiat Corporation. Elevated water and sewage lines prevent thaw of underlying permafrost. Buried, insulated utilidors are also used. Photo by Heath Sandall NARL = Naval Arctic Research Laboratory; ESRL = Earth System Research Laboratory..

distinguished cultural, commercial, military, and scientific history (Brower 1948; Sonnenfeld 1960; Arctic Institute of North America 1969; Norton 2001; Bockstoce 2009), including in permafrost research.

Urban Morphology

Utqiaġvik's compact, older urban core contains a mix of municipal buildings and small detached houses (Figure 2A). By the mid-twentieth century these structures had largely replaced sod huts (Figure 2B), which had provided thermal insulation and protected the underlying permafrost. New neighborhoods with larger houses have been developed since the 1970s near downtown. Current construction and plans for future expansion are mainly near Browerville, a neighborhood northeast of the urban core that exhibits a high-latitude adaptation of the sprawling suburban morphology (Figure 2C) found elsewhere in the United States (Duany, Plater-Zyberk, and Speck 2000; Klene, Nelson, and Hinkel 2013). Recently constructed buildings are elevated 1 to 2 m above the ground surface on pilings to prevent disruption of the ground thermal regime (Figure 2D), but many older homes have not been retrofitted with such construction (Figure 2E). Utility lines run in *utilidors*, insulated boxes that prevent freezing (Figure 2F).

Few buildings are more than two stories, even in the central business district. The low building heights and placement of many buildings atop pilings limits the "urban canyon" effects common in larger urban areas. Road networks are composed of 2-m-thick, graded sand and gravel berms that allow permafrost to aggrade within the bed and stabilize the surface (Hinkel, Klene, and Nelson 2004; S. W. Muller 2008). Roads interfere with local hydrology, particularly during spring runoff when water becomes trapped within the "grids" formed by intersecting berms (Figure 2C), and must be pumped out (Klene, Nelson, and Hinkel 2013). Blowing snow forms complex patterns of drift and scour zones within the city. Since 1997, several large snow fences have been constructed to reduce the amount of snow reaching the city (Hinkel, Bockheim, et al. 2003; Hinkel and Hurd 2006).

Physical Setting

Although cold, the Barrow Peninsula's climate is moderated by proximity to the Arctic Ocean. Snow

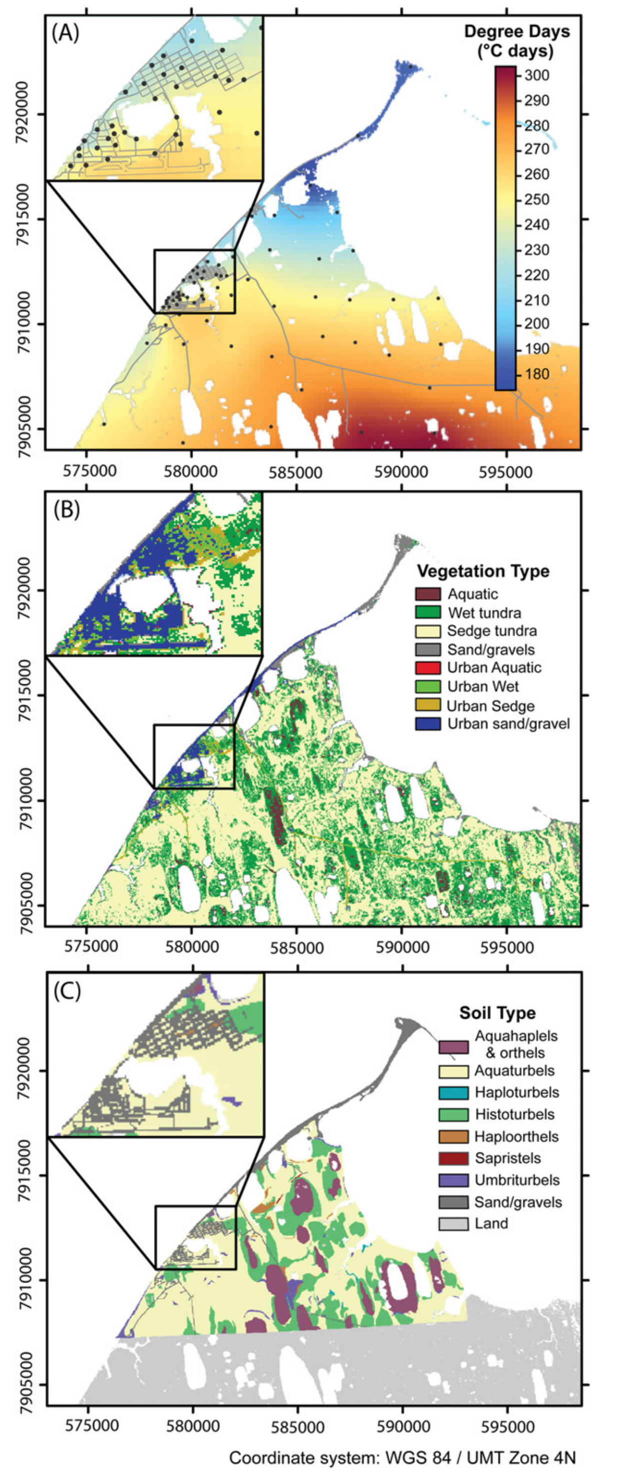

Figure 3. (A) Map of thawing degree-day totals measured across the study area, summer 2002. (B) Modified land-cover classification based on U.S. Bureau of Land Management (1998) analysis. Urban versions of each class were within 30 m (one pixel) of human infrastructure such as roads and buildings. Half of the sites are within the "urban" area and half in "rural" tundra. (C) Georeferenced soil map adapted from Bockheim et al. (1999), based on Drew (1957). Soil properties are shown in Table 2.

covers the ground from September or October through May or early June, with shore-fast sea ice from November to June or July. Mean February, July, and annual temperature normals (1981–2010) are –25.7, 4.9, and –11.2 °C, respectively (National Centers for Environmental Information 2018). Annual precipitation is low (115 mm), with the majority falling as rain in summer. The magnitude of the local winter urban heat island effect within the city averaged 2 °C over a four-year (2001–2005) period, occasionally reaching 6 °C (Hinkel and Nelson 2007). In summer, the area is affected strongly by maritime influences and no heat island effect is apparent (Figure 3A; Hinkel, Klene, and Nelson 2004).

Tundra vegetation in the Barrow Peninsula is a complex of sedge, grass, and moss wetlands (Figure 3B; Walker et al. 2002; CAVM Team 2003). Shallow thaw lakes cover 22 percent of the area and an additional 50 percent of the landscape is occupied by drained thaw-lake basins (Hinkel, Eisner, et al. 2003). A large volume of work was published in the 1970s about the variability of local land-cover types, based on research performed for the International Biome Program (IBP; e.g., Brown et al. 1980; Webber et al. 1980). The IBP sites have been resampled several times during the 1972 to 2010 period (Lara et al. 2012; Villarreal et al. 2012). Substantial functional changes have occurred since the baseline study was carried out. The changes were greatest in aquatic and wet plant communities and least in moist and dry communities.

Permafrost underlies the Barrow region to depths of 350 to 400 m and is considered ice rich, with ice content of 50 to 75 percent in the upper 2 m (Sellmann et al. 1975; Hinkel et al. 1996). Except in sandy and gravelly soils, maximum summer ALT in undisturbed areas rarely exceeds 50 cm (Nelson et al. 1998; Hinkel and Nelson 2003). Drained lake basins have greater depths of thaw than intervening areas of upland tundra. Soils of the Barrow region (Figure 3C) were described by Drew et al. (1958), Tedrow and Cantlon (1958), Brown (1967), Bockheim et al. (1999), and Bockheim, Hinkel, and Nelson (2001). All soils in this region are categorized in U.S. soil taxonomy as Gelisols, the definition of which specifies that permafrost occurs within 1 m of the surface, and that soil structure exhibits the effects of frost action (Bockheim et al. 1997).

Permafrost Research at Barrow

Long-term permafrost monitoring programs in the Barrow Peninsula have contributed substantially to development of geocryological theory. The initial permafrost temperature measurements in the area were made during the First International Polar Year (1882–1883) by the Ray Expedition (Ray et al. 1885; Barr 2008). In the mid-1940s, the U.S. Geological Survey (USGS) initiated a program of geothermal measurements that ultimately confirmed the effects of climatic warming on permafrost (Lachenbruch and Marshall 1969, 1986). Many other permafrost-related projects were conducted under the auspices of the Naval Arctic Research Laboratory (Brewer 1958; Arctic Institute of North America 1969; Norton 2001).

The U.S. Army's Cold Regions Research and Engineering Laboratory (USA CRREL) established a series of plots for active layer measurements in the 1960s (Brown and Johnson 1965; Brown 1969). Since the early 1990s, a series of projects funded by the U.S. National Science Foundation has expanded this active layer measurement program as a component of the Circumpolar Active Layer Monitoring (CALM) network (Brown, Hinkel, and Nelson 2000; Nelson et al. 2008; Shiklomanov et al. 2008; Shiklomanov et al. 2010).

A new program of borehole temperature measurements was initiated in 2000, when two deep boreholes were drilled and equipped with thermistor cables and data loggers (Yoshikawa et al. 2004). These sites are located within and adjacent to the Barrow Environmental Observatory (BEO) and, with several other long-term projects concerned with coastal erosion (Brown et al. 2003), plant phenology (Hollister et al. 2008), snow (Cox et al. 2017), and thaw subsidence (Lewellen 1972; Streletskiy et al. 2017), contribute to this permanent, protected observatory (Figure 1). Within the city limits, a program of thermal monitoring within ice cellars, underground chambers excavated in permafrost and used by local residents for storing harvested wildlife, has been carried out since 2005 (Nyland et al. 2017).

Since the early 1970s, a location adjacent to what is now the BEO has been a node in the National Oceanic and Atmospheric Administration's Earth System Research Laboratory (ESRL; formerly Climate Monitoring and Diagnostics Laboratories). This program monitors climate and atmospheric trace gases at a series of sites around the world

(ESRL 2016). Information about research on the BEO is available through the Next Generation Ecosystem Experiments Arctic Web site (Next Generation Ecosystem Experiments 2018).

Active-Layer Thickness

Patterns of near-surface temperature in the North Slope region can be complex and highly variable, even over short distances in relatively undisturbed parts of the landscape (Drew et al. 1958; Walsh 1977). Soil temperature measured within a series of 1-ha plots in the Kuparuk River Basin, 250 km east of the Barrow Peninsula (Klene et al. 2001), indicated that thawing degree-day sums at the interface between mineral soil and organic matter varied by as much as a factor of two. Strong and systematic relationships between air and mean soil surface temperature were, however, apparent in all of the natural land-cover classes examined when a density of five temperature sensors per plot was achieved. Soil moisture appeared to be the dominant factor responsible for variation within individual land-cover types (Klene et al. 2001). Karunaratne and Burn (2004) identified near-surface thermal diffusivity, which is strongly moisture dependent, as the primary factor controlling the summer n-factor (the ratio of temperature at the ground surface to that in the air) at five sites near Mayo, Yukon.

Records of ALT in the Barrow Peninsula extend back to the 1950s, albeit in discontinuous fashion (Shiklomanov et al. 2010; Brown et al. 2015). The geographic variability of ALT in northern Alaska can be substantial. Nelson et al. (1998) and Nelson, Shiklomanov, and Mueller (1999) found that on the coastal plain the greatest variations in ALT occur over lateral distances of 100 m and above, primarily due to soil moisture variations associated with the distribution of thaw-lake basins. A secondary peak, over distances of about 10 m, is associated with the spacing of ice-wedge polygons. In the foothills, maximum variability is controlled by microtopography and occurs over much smaller distances. Similar results were obtained by Gomersall and Hinkel (2001).

Methods for calculating ALT are often extensions of soil temperature models. They range from simple analytic solutions for frost and thaw depth using a small number of variables (e.g., Carlson 1952; Jumikis 1977) to complex numerical models (e.g., Nakano and Brown 1972; Waelbroeck 1993). The latter class of models can be difficult to implement over extensive regions because of the need to specify details of subsurface parameters and their variability.

Most discussions of urban effects on permafrost in the Arctic focus on a single structure and predict a thaw bulb around it (e.g., Lachenbruch 1957; Hwang 1976) or calculate effects over regional or hemispheric scales (e.g., Nelson, Anisimov, and Shiklomanov 2001; Streletskiy, Shiklomanov, and Nelson 2012; Hjort et al. 2018). Few studies have examined the effects that different degrees of development might have at local scales. Similarly, there has been little consideration of urban areas with morphologies more complex than a small, simple cluster of structures.

Outcalt and Goodwin (1980) examined potential urban effects using daily weather data from the National Weather Service (NWS) in Barrow to model the date of snowmelt and maximum ALT, among other factors, using a one-dimensional numerical scheme requiring fifteen input variables (Outcalt 1972). This simulation experiment examined the potential impacts of different surface modifications on snowmelt and thaw depth in a highly urbanized area containing a 2-m gravel and asphalt pad, snow removal, and building heights of 2 m, as well as a less-affected outlying area with decreased albedo from dark dust but no other modifications. The model predicted substantially increased ALT in the core urban area and more modest increases in the outlying areas. No validation data were available at the time of the study.

Methodology

Field Instrumentation

Seventy-one sites were instrumented with temperature loggers between June 2001 and August 2002 as part of the BUHIS (Hinkel, Nelson, et al. 2003; Klene, Hinkel, and Nelson 2003; Hinkel, Klene, and Nelson 2004; Hinkel and Nelson 2007). To account for greater variability within the urban area, half of the sites were located within the urbanized area and half within the much larger surrounding area of relatively undisturbed tundra (Figures 1, 3A). Each site was instrumented with a two-channel miniature data logger (Hobo Pro®, Onset Computer Corporation, Pocasset, Massachusetts) making simultaneous measurements of air (1.8 m height) and near-surface (5 cm depth) temperatures at hourly intervals. The data

Table 1. Vegetation classes in the Barrow area based on a U.S. Bureau of Land Management (1998) analysis of Landsat TM and SPOT imagery

Vegetation class	Description	Common species	Rural *n*-factor	Urban *n*-factor
Water	All water with less than 15% vegetation cover	None.	N/A	N/A
Aquatic	Water deeper than 10 cm, with up to 50% vegetation cover	Predominantly *Arctophilia fulva* and *Carex aquatilis*	1.00	1.10
Wet/flooded tundra	Areas with ephemeral shallow water 10 to 50%; polygonal and nonpatterned areas are included	*A. fulva*, *C.* spp., *Eriophorum* spp., *Hippuris vulgaris*, *Potentilla palustris*, *Sphagnum* spp., and *Salix* spp. on dry ridges	0.75	1.05
Sedge/grass meadow	Continuous layer of sedges and grasses with a moss/lichen understory; tussock tundra is included but only sporadically	*C. aqualtilis*, *Eriophorum* spp., *Arctagrostis latifolia*, and *Poa arctica*. *Cassiope* spp., *Ledum* spp., and *Vaccinium* spp. are found	0.75	1.25
Partially vegetated/barrens	Beach gravel, sand dunes, and developed or disturbed areas	Typically less than 10% of surface is vegetated. *Poa* spp., *Salix* spp., *Stellaria* spp., and *Astragulus* are occasionally found	1.60	2.00

Note: "Urban" versions of each class (those within 30 m of a road or building) were also defined. A summer *n*-factor was calculated for each land-cover category from measurements made at the Barrow Urban Heat Island Study study sites and rounded to the nearest 0.05.

loggers monitor temperatures from –50 °C to +30 °C and have an accuracy of ±0.2 °C and a precision of 0.02 °C at the freezing point. Sensors observing air temperature were housed in five-gill radiation shields (R. M. Young Co., Traverse City, Michigan).

Hourly air and soil measurements were processed into mean daily air and soil temperatures. Vegetation was classified within a 4-m^2 area surrounding the base of each mast. Depth of thaw was measured in June and August of each year using a calibrated metal rod to probe for the base of the active layer. Two measurements were made at each location and the mean of these paired observations was used in subsequent data analysis.

Air and Soil Temperature Fields

A summer air-temperature field was created by summing degree days between 1 June and 30 August 2002 at those sites with complete records for this time period and interpolating to a grid with 30-m node spacing. Kriging was used to interpolate because validation analysis showed that it was as accurate as several other methods used, while allowing estimation over the full extent of the study area (Hinkel, Klene, and Nelson 2004). A maritime influence dominates the summer pattern, with cooler temperatures in the northeast and warmer temperatures in the southern and western parts of the study area. An urban heat island effect was not detected in summer (Hinkel, Klene, and Nelson 2004; Hinkel and Nelson 2007).

Air temperature varies systematically across the study area in response to the maritime influence (Figure 3A). Near-surface soil temperature varies more dramatically (Klene, Nelson, and Hinkel 2013). The *n*-factor is used here as a surrogate measure to represent spatial variations in the heat exchange between the atmosphere and soil, based on the land-cover type at each site. The summer (thawing) *n*-factor is usually expressed as the ratio of thawing degree-days at the surface (DDT_s) to that in the air (DDT_a) and is frequently computed by summing mean daily warm-season temperatures. The *n*-factor was developed specifically for use with the Stefan solution for frost or thaw depth (Jumikis 1977) and homogeneous engineered surfaces as a method for addressing the thermal offset between surface and air temperature when surface temperature data are unavailable.

N-factors were calculated from BUHIS network data using the computational procedure outlined by Klene, Nelson, and Shiklomanov (2001) and Klene, Nelson, and Hinkel (2013) over the summer of 2002. Results were grouped by land-cover (vegetation) type (Table 1). "Urban" *n*-factors are larger in each case than corresponding *n*-factors for the "rural" land-cover class, as would be expected given the longer snow-free season in the city and other differences in the energy balance.

The Modified Berggren Solution

The widely used Stefan solution (e.g., Jumikis 1977) overestimates depths of both freezing and thawing in most circumstances, in part because it disregards the effects of heat capacity in the substrate. Estimates were made in the ALT mapping applications performed by Nelson et al. (1997) and Klene, Nelson, and Shiklomanov (2001) using regression-based or semiempirical procedures, respectively, which counterbalanced those qualities of the Stefan solution producing overestimates.

Numerous strategies for improving the accuracy of Stefan estimates have been developed (Lunardini 1981), the most common of which has come to be known as the modified Berggren solution. Introduced by Berggren (1943) and improved substantially through the work of Aldrich and Paynter (1953, 1966), this solution to the general frost/thaw-depth problem reduces predicted frost/thaw penetration by accounting for the effects of volumetric heat capacity. A brief history of the Berggren solution's development was provided by Paynter (1999). Variants of the modified Berggren solution continue to be used widely by engineers (e.g., Smith and Rager 2002; Andersland and Ladanyi 2004) but have not been employed previously to calculate spatial fields of freezing or thawing depths.

The modified Berggren solution for the depth of freezing or thawing (e.g., Andersland and Ladanyi 2004) is given for the thawing case by

$$z_t = \lambda\sqrt{\frac{2k_t s(n_t DDT_a)}{\rho w L}}, \tag{1}$$

where z_t is ALT (m), k_t is thermal conductivity of the soil for the thawed state (J s^{-1}m^{-1}°C^{-1}), s is a scaling factor (86,400 s day^{-1}), n_t is the dimensionless thawing *n*-factor, DDT_a is the seasonal air degree-day sum (°C days), ρ is soil density (kg m^{-3}), w is the fraction by weight of the soil's water content (dimensionless), L is the latent heat of fusion (J kg^{-1}), and λ is a coefficient accounting for the heat required to raise the temperature of the soil. The difference between the Berggren and Stefan solutions is the inclusion of the λ coefficient in the former, the net effect of which is to reduce the magnitude of predicted frost and thaw depth (Aldrich and Paynter 1953), thereby improving the accuracy over that of simpler forms of the Stefan solution. Several methods for calculating the λ coefficient have been developed. Most textbook examples (e.g., Andersland and Ladanyi 2004) incorporate a series of graphs because the most common computation schemes make use of complex error functions. Zarling, Braley, and Pelz (1989) developed a set of equations, based on work by Lunardini and Varotta (1981) and Grigull and Sandner (1984) and denoted by λ', that do not include the error function but produce results in the midrange of the six versions of the modified Berggren solution they compared to predict frost penetration and thaw depth. Their formulation for λ' is given as

$$\lambda' = \frac{-\gamma + \sqrt{\gamma^2 + 2a\pi}}{a\sqrt{2\pi Ste}}, \tag{2a}$$

where

$$\gamma = \sqrt{\frac{k_f c_f}{k_t c_t} \times \left(\frac{T_f - \bar{T}_i}{\overline{T_s} - T_f}\right)}, \tag{2b}$$

$$Ste = c_t \frac{\overline{T_s}}{L}, \tag{2c}$$

and

$$a = \frac{1}{Ste} + \frac{1}{3} + \frac{2\gamma}{\pi}. \tag{2d}$$

$\overline{T_s}$ is the summer mean soil surface temperature (°C), T_f is the freezing point (0 °C), $\overline{T_i}$ is the mean annual soil surface temperature (°C), k_f is the thermal conductivity of the frozen soil (J s^{-1} m^{-1} °C^{-1}), c_f and c_t are the volumetric heat capacity of the frozen and unfrozen soil, respectively (J m^{-3} °C^{-1}), and other variables are as in Equation 1.

Several additional input variables are required to employ the modified Berggren solution in a geographic context. These include an empirical *n*-factor for each land-cover class (Klene, Nelson, and Shiklomanov 2001); a raster land-cover map of the

Table 2. Characteristics of soil classes used in calculations

U.S. soil class to subgroup	Soil texture[a]	Bulk density[b] (kg m^{-3})	Thawed thermal conductivity[c] (W m^{-1} K)	Frozen thermal conductivity[c] (W m^{-1} K)	Thawed heat capacity[i] (kJ m^{-3} K)	Frozen heat capacity[i] (kJ m^{-3} K)	Soil moisture[d] (% volumetric, % mass)	Area[e] (%)	Drew's soil class
Aquorthels	Silty clay	1,000	0.85	2.36	3,263	2,008	60, 60	8.6	Normal half bog
Aquiturbels[h]	Silty clay loam	800	0.57	1.26	1,774	1,188	35, 40	52.9	Normal meadow and upland tundra
Haploturbels	Silty clay	1,250	0.86	1.16	2,249	1,595	25, 21	0.2	Dry upland tundra
Histoturbels	Loam	800	0.62	1.73	2,276	1,439	50, 56	21.9	Wet meadow tundra
Haplorthels (Umbrorthels)[g]	Loamy sand	850	0.54	0.94	1,529	1,085	25, 28	<0.1	Arctic brown
Sapristels	Silty clay	300	0.33	1.34	853	540	50, 77	1.0	Dry half bog
Umbriturbels (Hemistels)[g]	Clay loam	1,000	0.64	1.00	1,799	1,276	25, 25	2.0	Dry meadow tundra
Psammorthels	Loamy sand	1,700[f]	1.22	0.76	1,636	1,458	5, 4	4.4	Gravel

Note: Water covered 9% of the mapped area.
[a]Averages calculated from profiles described in Bockheim, Hinkel, and Nelson (2001), Table 3, and soil texture chart.
[b]Bockheim et al. (1999), Table 3.
[c]Thermal conductivity k (W m^{-1} K) was estimated using Kersten's (1949) formulation for soils with <50% sand, based on dry density d (expressed in g cm^{-3}) and soil moisture w (% by mass), using the equation $k = 0.1442 * (0.9 \log w - 0.2) * 10^{0.625d}$. The sand equation was used to calculate Psammorthels category.
[d]Estimated from relative wetness in Bockheim et al. (1999) descriptions; converted using given bulk densities.
[e]Bockheim, Hinkel, and Nelson (2001), Table 2.
[f]J. G. Bockheim, personal communication (2005).
[g]Bockheim, Hinkel, and Nelson (2001).
[h]Average of two sample cores in Bockheim et al. (1999).
[i]Zarling, Braley, and Pelz (1989).

area to determine which n-factor to use (Figure 3B), an air temperature field, expressed as seasonal degree-day totals (Figure 3A); and a raster soils map with corresponding estimates of soil properties for each type (Figure 3C and Table 2). Values of thermal conductivity for frozen soils were estimated from equations representing Kersten's (1949) data. Heat capacity was estimated following the procedures of Zarling, Braley, and Pelz (1989), as represented in Equation 2. These parameters were determined for each soil class (Table 2). Although snow cover exerts an important control over winter soil temperature (Goodrich 1982; Gisnas et al. 2016), information was not available on its spatial distribution for the winter of 2001–2002. To include snow-cover effects in a general manner, a simple mean winter soil surface temperature (–9.58 °C) was calculated from all of the BUHIS sites for which records were available for the period 1 September 2001 to 31 May 2002. This estimate was used to calculate mean annual soil surface temperature for Equation 2b.

Land-Cover and Soils Maps

Although several recent maps depicting land-cover types (Lara et al. 2015; Andresen et al. 2017) are available for the area, the U.S. Bureau of Land Management's (1998) map of the National Petroleum Reserve-Alaska (NPRA) was used in this study because it (1) employed a commonly used land-cover classification scheme when classifying the BUHIS sites as they were installed and (2) is of a vintage similar to the data collected for this study, an important consideration in this dynamic environment (Figure 3B). This map, which covers the entire 90,000-km^2 NPRA, was produced by the USGS using a combination of eight Landsat Thematic Mapper and three SPOT scenes obtained between 1990 and 1998. The seven classes were reduced, based on knowledge of the Barrow area, to five categories (water, aquatic, wet, sedge meadow, and barrens) to correct consistent misclassifications in the study area (Table 1; also see Klene, Nelson, and Hinkel 2013). A collection of geographic information system (GIS) data layers, obtained from the North Slope Borough GIS office (Barrow Area Information Database 2018), was used to define an infrastructure-rich "urban area" surrounded by a 30-m buffer zone. The width of the buffer corresponds to the pixel size of the land-cover imagery and represents the distance in which 95 percent of road dust deposition takes place (Walker and Everett 1987). Buffer width is approximately twice the diameter of local ice-wedge polygons, which can introduce fine-scale variability in ALT (Nelson, Shiklomanov, and Mueller 1999; Fagan and Nelson 2017). All pixels within the buffered area were classified as belonging to the "urban" portion of each land-cover category. Further details are provided in Klene, Nelson, and Hinkel (2013).

Data from the BEO and the BUHIS sites (Figure 1) were used to validate the land-cover classification (Figure 3B). Overall accuracy was 49 to 60 percent against two validation data sets (Klene, Nelson, and Hinkel 2013), after correction for systematic errors. This limited correspondence might be attributable to the large amount of heterogeneity within the tundra near the city (Stow et al. 2004) and in the coastal plain in general. Thirty-meter resolution imagery obviously cannot capture microsite characteristics within and between polygonized ground in this region, for instance. Moreover, the land-cover classification was performed over a much larger area and was not field-checked near Barrow. Geographic heterogeneity in the urban area is even greater than that in the rural area. Localized clusters of vegetation associations and cultural features (i.e., rooftops, vehicles, baleen) contribute to variability.

Drew's (1957) map of soils in the Barrow area was reclassified by Bockheim et al. (1999) using contemporary soil taxa corresponding to the Gelisol order of U.S. soil classification. Bockheim's map has eight soil classes (Figure 3C). A digital version of Bockheim's map was overlain on a USGS base map (USGS 1955) produced from aerial photos of a vintage similar to those used by Drew (1957). A series of landscape changes (thaw lake drainage and road construction) occurred around Barrow between when the soils map was originally prepared and the fieldwork for this study was done, and modifications were made to account for these (A. E. Klene unpublished data). Empirically based estimates of soil thermal properties are available for several locations near Barrow in different soil types (Lord, Pandolfo, and Atwater 1972; Nakano and Brown 1972; McGaw, Outcalt, and Ng 1978; Outcalt, Gray, and Benninghoff 1989). Use of these other sources in conjunction with the soils map (Figure 3C) allowed development of estimated soil properties for each new soil class (Table 2).

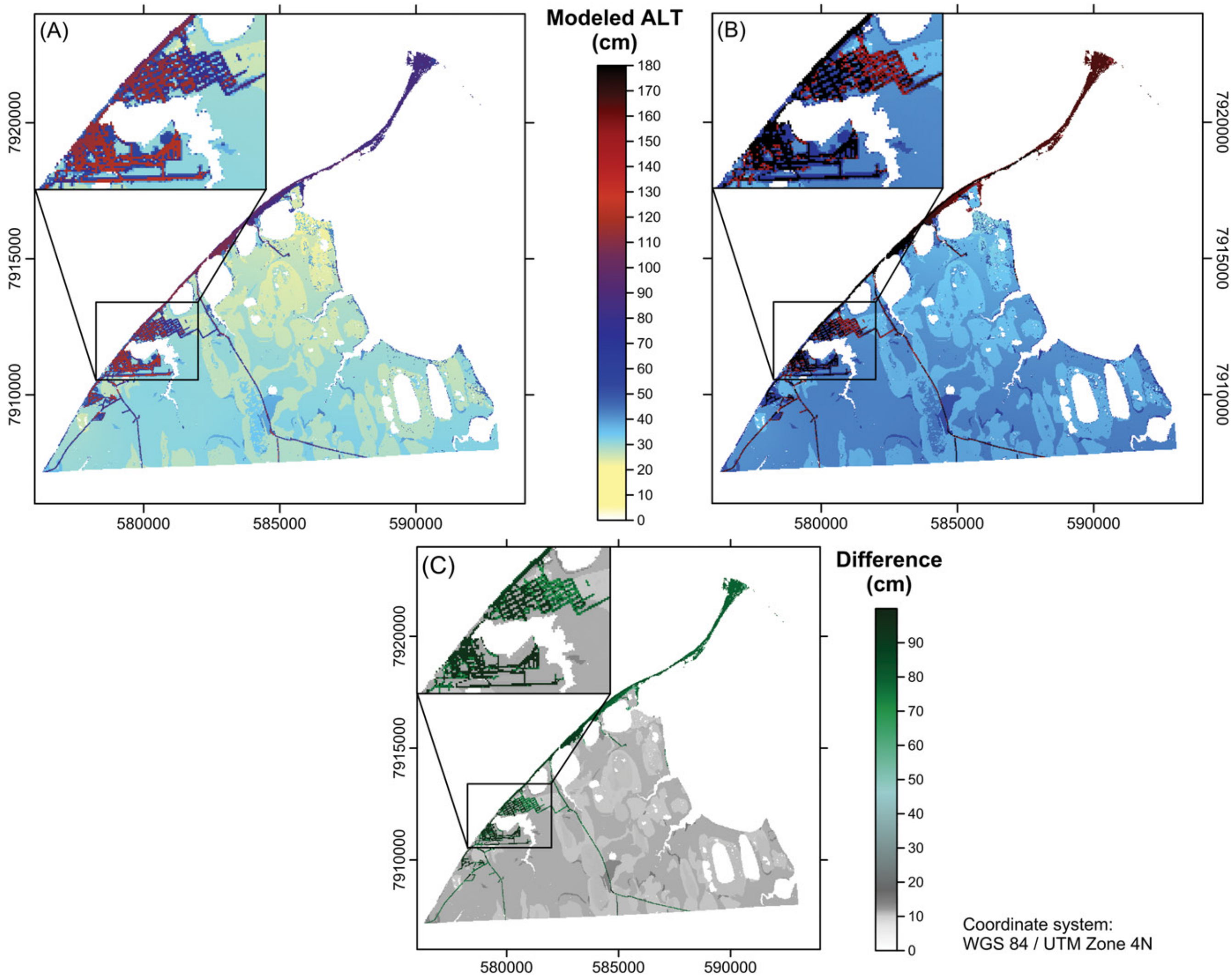

Figure 4. ALT maps for August 2002, created using digital representations of the empirical degree-day map (Figure 3A), the land-cover map (Figure 3B), empirical *n*-factors (Table 1), and the soils map (Figure 3C and Table 2). (A) ALT map created using the modified Berggren solution (Equations 1–2). (B) ALT map created using the basic Stefan solution (Equation 1 without λ coefficient). (C) Difference map based on the matrix **D**, produced by the operation **D = S − B**, where **S** and **B** are matrices of ALT values produced by the Stefan and Berggren solutions, respectively. ALT = active-layer thickness.

Results

Active-Layer Maps

A map of end-of-season ALT for 2002 (Figure 4A) was constructed using the Berggren solution with empirical air and soil temperature data from BUHIS sites, a land-cover map incorporating a variety of natural and built environments, a map of estimated soil properties, and winter temperatures within the modified Berggren solution, as described by Equation 2. For comparative purposes, a map based on the simple Stefan solution was also constructed using the same data sources (Figure 4B). Figure 4C is a difference map, computed by subtracting the matrix of Berggren values from that of the Stefan map.

Each input field exerts a discernible effect on the ALT maps. Deep thaw penetration in the sand and gravel comprising the road network and other infrastructure elements is readily apparent in both the Berggren and Stefan maps and represents the maximum values of ALT in the study area. Owing to neglect of volumetric heat capacity in the Stefan formulation, ALT extends to unrealistic depths in these parts of Figure 4B.

The effect of a general trend of cooler air temperature in the northeast to warmer temperature in the south-central part is also apparent (cf. Figures

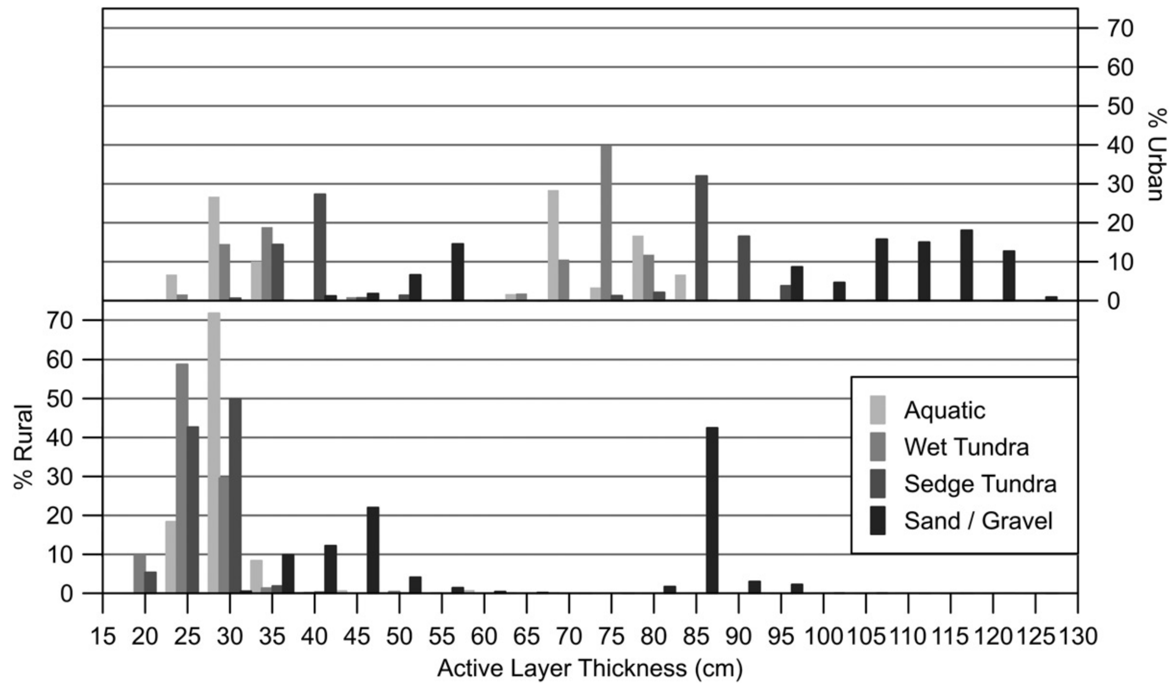

Figure 5. Histogram of the percentage of each of the urban (top) and rural (bottom) land-cover classes in 5-cm bins of active-layer thickness.

3A and 4A). Vegetation differences are distinct within individual thaw-lake basins, reflecting differences in the moisture regimes between the shelves and centers of the former lake bottoms. Similar soil types connect some of the thaw-lake basins.

Striking differences are apparent in the predicted range and distribution of values in the "rural" and "urban" portions of the study area (Figures 4A and 5). ALT values in the undisturbed aquatic, wet, and sedge tundra categories were predicted to be 21 to 71 cm, whereas the urban aquatic, wet, and sedge tundra categories were 28 to 95 cm, with minimums in each urban category 3 to 12 cm deeper than their respective rural class and maximums 17 to 37 cm deeper. Thaw depths predicted in rural sand and gravel ranged from 34 to 106 cm, whereas the urban sand and gravel was estimated to be 42 to 126 cm.

A bimodal distribution of ALT values exists in the rural sand and gravel land cover and in all urban categories (Figure 5). Examining ALT by soil category, only thirty pixels had depths over 60 cm and none above 71 cm except for sand and gravel, which had no estimates below 52 cm. Some pixels have sand and gravel as both the land-cover class and the soil category, whereas others do not.

Although it is not unusual to observe tundra vegetation growing atop sand and gravel pads in the urbanized area or to observe a thin layer of sand and gravel atop another soil type, such a circumstance can arise as an artifact of the process used to create the input layers. The road network was overlain on the soils map and those pixels were recategorized as sand and gravel soils. For the satellite-derived land-cover map, however, the road networks were used to define the urban pixels and the category was not changed to sand and gravel. Sand and gravel soils thaw deeper and in all land-cover categories underlain by those soils were predicted to have deeper ALT. Thus, in Figure 4A, rural gravel had peaks in ALT at about 45 and 85 cm, and all of the urban land-cover categories have similar curves. The increased range and the bimodality predicted in the urban categories are consistent with observations made during the BUHIS study. Including such fine-scale variability accurately could enrich efforts to map permafrost-related phenomena such as carbon storage (e.g., Olefeldt et al. 2016).

Compared with the map of ALT based on the Stefan solution (Figure 4B), inclusion of volumetric heat capacity in the Berggren ALT map (Figure 4A) produced substantially reduced ALT values, subdued the differences between vegetation classes, and imparted greater continuity between locations with different soil categories. The accuracy of predicted ALT in gravel berms was improved substantially from the overestimates yielded by the Stefan

Table 3. Validation of ALT, August 2002

Land cover	Number of observations	Mean measured ALT (cm)	Mean estimated ALT (cm)	Mean difference (cm)
CALM grid	114	30.6	27.2	–3.4
MSU BEO	596	26.4	28.6	2.2
BUHIS rural	26	29.3	35.0	5.8
BUHIS urban	28	62.4	81.1	19.0

Note: Measured and estimated values (cm) at the BEO CALM grid, those collected by MSU personnel on the BEO, and from the BUHIS sites. The CALM and MSU data are from relatively undisturbed areas, whereas the BUHIS data are separated into urban and rural. ALT = active-layer thickness; CALM = Circumpolar Active Layer Monitoring; MSU = Michigan State University; BEO = Barrow Environmental Observatory; BUHIS = Barrow Urban Heat Island Study.

Table 4. Measured and estimated end-of-season ALT values from the Berggren solution for 2002 at the BUHIS sites by land-cover category

Land cover	Number of observations	Mean measured ALT (cm)	Mean estimated ALT (cm)	Mean difference (cm)
Aquatic	3	26.0	28.8	4.5
Wet tundra	3	27.0	28.6	–1.8
Sedge meadow	18	26.3	34.5	9.3
Gravel	2	80.7	58.5	–12.5
Urban aquatic	2	70.0	71.8	1.8
Urban wet	9	44.0	73.2	29.2
Urban sedge	7	60.0	96.7	36.7
Urban gravel	10	81.1	79.7	1.1

Note: Values were calculated from all available BUHIS observations. Classification of 11 validation points within the study area as water by the vegetation map prevented calculation of a difference between estimated and observed at those locations. ALT = active-layer thickness; BUHIS = Barrow Urban Heat Island Study.

solution. Visible differences between locations with contrasting moisture regimes within drained thaw-lake basins were lessened. The large volumetric heat capacity of the Aquaorthels (Table 2) surrounding lake basins constrains ALT in these soils, yielding more realistic values than those produced by the Stefan formulation. The difference map (Figure 4C) highlights these contrasts in mapped results.

Validation

ALT was measured at each of the BUHIS sites where air and soil temperatures were obtained. Additional observations were available from the Barrow CALM grid, a surveyed 1 × 1 km plot on the BEO where end-of-season ALT measurements are made annually (Hinkel and Nelson 2003; Nelson et al. 2008; Fagan and Nelson 2017). Another 750 ALT measurements were available for the BEO from the former Michigan State University (MSU) Arctic Ecology Laboratory, collected during a vegetation classification accuracy assessment in August 2002 (C. E. Tweedie, personal communication; Table 3).

Table 3 shows mean ALT results obtained from the three validation data sets. ALT was underestimated on the CALM grid by 3.4 cm (–11.1 percent) and overestimated at the MSU/BEO sites by 2.2 cm (+8.3 percent). The Berggren solution overestimated the BUHIS rural sites by an average of 4.0 cm (+12.9 percent) and the BUHIS urban sites by 17.4 cm (+27 percent). Table 4 shows errors according to BUHIS land-cover categories. The Berggren solution underestimated the natural gravel category by 12.5 cm (–12 percent) and overestimated natural sedge by 9.3 cm (+18.4 percent), whereas the other two classes are within 5 cm. In the urban classes, only urban wet tundra and urban sedge meadow are in error by more than 2 cm. Ranges in each category were similar between observed and predicted (Table 4).

The numbers reported here are class means. Values at point locations could be quite different, owing to variation in the parameters used in the formulation, as well as in other influences that have only affected specific sites, particularly in the urban environment. Biases, both systematic and unsystematic, occur in the urban land-cover classes. This could be attributable to any of several factors, such as hydrological patterns found in the urbanized area (Hinkel, Klene, and Nelson 2004).

There are several possible explanations for differences between observed and predicted values, including the use of n-factors based on relatively few study sites, land-cover or soils misclassification, inadequate spatial resolution in the urban areas, and lack of sufficient complexity in the model to capture the vertical stratigraphy in the urban region. Sample sizes are low in several of the land-cover categories and future studies should stratify the sampling design more effectively. The fact that overestimation is increased at the BUHIS sites rather than the MSU BEO and CALM sites indicates that it is related not just to the urban effect but also to the scale of the land-cover classification, which was constructed at a more detailed level in the BUHIS sites but made comparisons with the land-cover map more difficult.

This project produced data that can also be used to make rough comparisons with Outcalt and Goodwin's (1980) predictions about infrastructure-induced changes in ALT. Their nonurban estimate of 35 cm is very similar to values observed at the rural sites and predicted using the Berggren solution. Their core urban estimate of 64 cm is in the mid-range of the urban predictions from the Berggren solution. In both cases, they are substantially lower than estimates from the simple Stefan solution.

Liu et al. (2015) and Schaefer et al. (2015) used interferometric synthetic aperture radar to infer 2006–2007 ALT from remotely sensed seasonal surface subsidence measurements in the Barrow area. Their ReSALT (remotely sensed active layer thickness) field shows some similarities with the Berggren ALT field produced in this study, with relatively homogeneous areas of low ALT values in drier sections of the rural Barrow Peninsula. Their maps did not resolve ALT in the urbanized area meaningfully, had systematic underestimates along the western and eastern portions of our mapped area, and overestimated ALT in some drained lake basins and around landfill sites. The Berggren solution yielded much higher accuracy in the urbanized area and in rural gravels, such as the beach ridge bisecting the CALM site (cf. Table 4; Nelson et al. 1998; Schaefer et al. 2015). The Berggren solution could be used to provide critical improvements in products derived from remotely sensed data, particularly in urbanized areas.

Conclusions and Recommendations

Substantial increases in the magnitude and heterogeneity of ALT result from urbanization. The large values and abrupt variations of ALT associated with Barrow's urban mosaic are striking at the local scale employed in this study (Figure 4A). Field collection of ALT data in such environments is, however, extremely consumptive of time and resources. Results from this study indicate that, given the availability of adequate soils, land use, and climate databases, advanced analytic models such as the Berggren solution can yield accurate depictions of ALT fields, even in very heterogeneous urban developments. At regional scales, accounting for the effects of urbanization will cause population centers to stand out as "hot spots" in ALT fields. Neglecting urban influences in regional models could result in substantial underestimates of the total volume of thawed soil in a region (Nelson et al. 1997).

Although this exploratory study did not achieve the degree of accuracy obtained from mapping experiments in natural landscapes of northern Alaska (Nelson et al. 1997; S. V. Muller et al. 1998; Shiklomanov and Nelson 1999), the results are encouraging by virtue of demonstrating that an advanced analytic solution to the frost/thaw-depth problem can be used effectively in local-scale urban mapping applications involving abrupt changes in land cover and material properties. Yi et al. (2014) found this class of models to also be effective in discerning differences in the thermal regimes beneath point locations in various microtopographic elements of ice-wedge terrain, and this result could be incorporated into mapping procedures. The modified Berggren solution performed well for estimating mean values of ALT in land-cover classes within the rural and urban areas. Compared to the Stefan solution, it provides substantially improved estimates. Given the ambiguities and generalization in the land-cover classification and soils maps used in this study, the performance of the modified Berggren solution is promising for use in urban environments and generally as a vehicle for mapping ALT. The Berggren solution can also be used to improve the accuracy of ALT fields derived from remotely sensed data.

As development increases in Arctic regions, information about interactions between urban influences and ALT becomes vital, particularly given the increasing temperatures and potential for thaw subsidence accompanying climate change (Shiklomanov et al. 2013; Streletskiy et al. 2017). Calculations using estimated air temperature increases could be performed with the type of model used in this study to predict future thaw scenarios in other North Slope communities and elsewhere in the Arctic.

Improved land-cover classifications (e.g., Lara et al. 2015; Andresen et al. 2017; Lara et al. 2018), a validated soils map, and the high (2 m) resolution afforded by the Arctic digital elevation model (Polar Geospatial Center 2018) could improve the performance of the modified Berggren solution in the Barrow area and extend its application to other regions. Use of the multilayer version of the Berggren solution (Lunardini 1981) could also result in improvements to accuracy, particularly in the urbanized area if appropriate soils data are available. Used in conjunction with GIS-based methods for evaluating such parameters as bearing capacity (Streletskiy, Shiklomanov, and Nelson 2012), the approach employed here can provide useful characterizations of the suitability of specific locales for construction of settlements and industrial complexes, or for other types of planned development such as urban parks (e.g., Esau and Miles 2016).

Acknowledgments

We thank Ken Hinkel (Michigan Technological University) for collegial advice and for access to BUHIS data, Craig Tweedie (University of Texas at El Paso) for access to the MSU ALT data, and Jim Bockheim (University of Wisconsin–Madison) for soils data. Ron Paetzold and Cathy Seybold (U.S. Natural Resources Conservation Service, Lincoln, Nebraska) provided data from several installations in the Utqiaġvik (Barrow) area. We are grateful for logistical support from the Barrow Arctic Science Consortium, the Ukpeagvik Iñupiat Corporation, Barrow Utilities and Electrical Cooperative, Inc., public radio station KBRW, Michigan State University's former Arctic Ecology Lab, the North Slope Borough, and the residents and institutions of Utqiaġvik who graciously allowed us to conduct observations on their properties. Figures 1, 3, and 4 were substantially improved by Kevin McManigal (University of Montana) and Brianna Rick (Colorado State University). Steven Kazlowski (Left Eye Productions, Kingston, Washington), Nikolay Shiklomanov (George Washington University), and Heath Sandall (Fairbanks, Alaska) contributed photos to Figure 2. Jerry Brown (Falmouth, Massachusetts) provided an in-depth review while the article was in draft form. We are grateful to two anonymous reviewers for incisive assessments and useful suggestions.

Funding

Elements of this research were supported by the U.S. National Science Foundation (NSF), Grants OPP-0095088, OPP-0352958, OPP-0856421, ARC-1002119, and PLR-1304555, and University of Delaware Graduate Fellowships to Anna E. Klene. Any opinions, findings, conclusions, or recommendations expressed in this study are those of the authors and do not necessarily reflect the views of the NSF or any of the individuals named. Mention of specific product names does not constitute endorsement by NSF.

Note

1. The name change from Barrow to Utqiaġvik, decided by a narrow margin in a 2016 city election, was upheld through litigation in late 2017 and has been adopted by local, state, and federal agencies (Oliver 2017). Scientific research in the Barrow Peninsula has a very long history and a voluminous literature; however, the vast majority of it is associated with the name Barrow. To foster scientific continuity and avoid confusion, in this article we retain the name Barrow with reference to scientific research.

References

Aldrich, H. P. J., and H. M. Paynter. 1953. First interim report, analytical studies of freezing and thawing in soils. Technical Report 42, Arctic Construction and Frost Effects Laboratory, Hanover, NH.

———. 1966. Depth of frost penetration in non-uniform soil. U.S. Army Cold Regions Research and Engineering Laboratory Special Report 104.

Andersland, O. B., and B. Ladanyi. 2004. *An introduction to frozen ground engineering*. Hoboken, NJ: Wiley.

Andresen, C., M. J. Lara, C. E. Tweedie, and V. L. Lougheed. 2017. Rising plant-mediated methane emissions from Arctic wetlands. *Global Change Biology* 23 (3):1128–39. doi:10.1111/gcb.13469.

Anisimov, O. A., N. I. Shiklomanov, and F. E. Nelson. 1997. Global warming and active-layer thickness: Results from transient general circulation models. *Global and Planetary Change* 15 (3–4):61–77.

Anisimov, O. A., D. G. Vaughan, T. Callaghan, C. Furgal, H. Marchant, T. Prowse, H. Viljalmasson, et al. 2007. Polar regions. In *Climate change: Impacts, adaptation, and vulnerability. The contribution of Working Group II of the Intergovernmental Panel on Climate Change fourth assessment review*, eds. M. Parry, O. Canziani, J. Palutikof, P. van der Linden, C. Hanson, 653–85. Cambridge, UK: Cambridge University Press.

Arctic Institute of North America. 1969. The U.S. Naval Arctic Research Laboratory, Barrow, Alaska. *Arctic* 22:169–364.

Barr, W. 2008. *The expeditions of the first international polar year 1882–1883*. Calgary, AB, Canada: The Arctic Institute of North America.

Barrow Area Information Database. 2018. Accessed February 18, 2018. http://barrowmapped.org//.

Berggren, W. P. 1943. Prediction of temperature distribution in frozen soils. *Transactions, American Geophysical Union* Part 3 (11):71–77.

Bockheim, J. G., L. R. Everett, K. M. Hinkel, F. E. Nelson, and J. Brown. 1999. Soil organic carbon storage and distribution in arctic tundra, Barrow, Alaska. *Soil Science Society of America Journal* 63 (4):934–40.

Bockheim, J. G., K. M. Hinkel, and F. E. Nelson. 2001. Soils of the Barrow region, Alaska. *Polar Geography* 25 (3):163–81.

Bockheim, J. G., C. Tarnocai, J. M. Kimble, and C. A. S. Smith. 1997. The concept of gelic materials in the new Gelisol order for permafrost-affected soils. *Soil Science* 162 (12):927–39.

Bockstoce, J. R. 2009. *Furs and frontiers in the far North: The contest among native and foreign nations for the Bering Strait fur trade*. New Haven, CT: Yale University Press.

Bodhaine, B. A., J. M. Harris, and G. A. Herbert. 1981. Aerosol light scattering and condensation nuclei measurements at Barrow, Alaska. *Atmospheric Environment* 15 (8):1375–89.

Brewer, M. C. 1958. Some results of geothermal investigations of permafrost in Northern Alaska. *Transactions, American Geophysical Union* 39 (1):19–26.

Brower, C. D. 1948. *Fifty years below zero: A lifetime of adventure in the far North*. London: The Travel Book Club.

Brown, J. 1967. Tundra soils formed over ice wedges, northern Alaska. *Soil Science Society of America Journal* 31 (5):686–91.

———. 1969. Soil properties developed on the complex tundra relief of Northern Alaska. *Biuletyn Peryglacjalny* 18:153–67.

Brown, J., O. Ferrians, J. J. J. A. Heginbottom, and E. S. Melnikov. 1997. *International Permafrost Association circum-Arctic map of permafrost and ground ice conditions*. Scale 1:10,000,000, Circum-Pacific Map Series, Map CP-45. Reston, VA: U.S. Geological Survey.

Brown, J., K. M. Hinkel, and F. E. Nelson. 2000. The Circumpolar Active Layer Monitoring (CALM) program: Historical perspectives and initial results. *Polar Geography* 24:165–258.

Brown, J., and P. L. Johnson. 1965. Pedo-ecological investigations at Barrow, Alaska. CRREL Technical Report 159, U.S. Army Cold Regions Research and Engineering Laboratory, Hanover, NH.

Brown, J., M. Jorgenson, T. O. P. Smith, and W. Lee. 2003. Long-term rates of erosion and carbon input, Elson Lagoon, Barrow, Alaska. In *ICOP 2003 permafrost: Proceedings of the 8th International Conference on Permafrost*, ed. M. Phillips, S. M. Springman, and L. U. Arenson, 101–6. Amsterdam: A. A. Balkema.

Brown, J., P. C. Miller, L. L. Tiezen, and F. L. Bunnell. 1980. *An Arctic ecosystem: The coastal tundra at Barrow, Alaska*. Stroudsburg, PA: Dowden, Hutchenson & Ross.

Brown, J. M., F. E. Nelson, V. E. Romanovsky, C. Seybold, R. D. Hollister, and C. E. Tweedie. 2015. Long-term observations of active layer thawing and freezing, Barrow, Alaska. Paper presented at the Seventh Canadian Permafrost Conference, Québec, Canada, September 20–23.

Burn, C. R., and F. E. Nelson. 2006. Comment on "A projection of severe near-surface permafrost degradation during the 21st century" by David M. Lawrence and Andrew G. Slater. *Geophysical Research Letters* 33:L21503. doi:10.1029/2006GL027077.

Carlson, H. 1952. Calculation of depth of thaw in frozen ground, In *Special report 2: Frost action in soils: A symposium*, 192–223. Washington, DC: Highway Research Board.

CAVM Team. 2003. Circumpolar arctic vegetation map Scale 1:7,500,000. Conservation of arctic flora and fauna (CAFF) Map No. 1, U.S. Fish and Wildlife Service, Anchorage, AK.

Cox, C. J., R. S. Stone, D. C. Douglas, D. M. Stanitski, G. J. Divoky, G. S. Dutton, C. Sweeney, J. C. George, and D. U. Longenecker. 2017. Drivers and environmental responses to the changing annual snow cycle of Northern Alaska. *Bulletin of the American Meteorological Society* 98 (12):2559–77.

Daanen, R. P., T. Ingeman-Nielsen, S. S. Marchenko, V. E. Romanovsky, N. Foged, M. Stendel, J. H. Christensen, and K. H. Svensen. 2011. Permafrost degradation risk zone assessment using simulation models. *The Cryosphere Discussions* 5: 1021–1053. doi: 10.5194/tcd-5-1021-2011.

Dement'ev, A. I., L. A. Meyster, B. N. Dostovalov, N. A. Tsytovich, Z. A. Nersesova, E. P. Shusherina, and N. K. Pekarskaya. 1959. Metody inzhenerno-geokriologiicheskikh issledovanii [Methods of investigations in engineering geocryology]. In *Principles of geocryology. Part II, Engineering geocryology*, ed. V.A. Obruchev Institute of Permafrost Studies, 298–347. Moscow: Academy of Sciences of the U.S.S.R.

Drew, J. V. 1957. A pedologic study of Arctic coastal plain soils near Point Barrow, Alaska. Doctoral dissertation, Rutgers University, New Brunswick, NJ.

Drew, J. V., J. C. F. Tedrow, R. E. Shanks, and J. J. Koranda. 1958. Rate and depth of thaw in Arctic soils. *Transactions, American Geophysical Union* 39 (4):697–701.

Duany, A., E. Plater-Zyberk, and J. Speck. 2000. *Suburban nation: The rise of sprawl and the decline of the American dream*. New York: North Point Press.

Earth System Research Laboratory. 2016. Summary report 2004-2013, No. 28, Earth System Research Laboratory, Global Monitoring Division NOAA, Boulder, CO.

Esau, I., and V. Miles. 2016. Warmer urban climates for development of green spaces in northern Siberian cities. *Geography Environment Sustainability* 9 (4): 48–62 doi:10.15356/2071-9388_04v09_2016_04.

Fagan, J. E., and F. E. Nelson. 2017. Sampling designs in the Circumpolar Active Layer Monitoring (CALM) program. *Permafrost and Periglacial Processes* 28 (1): 42–51. doi:10.1002/ppp.1904.

Gisnas, K., S. Westermann, T. V. Schuler, K. Melvold, and B. Etzelműller. 2016. Small-scale variation of snow in a regional permafrost model. *The Cryosphere* 10:1201–15. doi:10.5194/tc-10-1201-2016.

Gomersall, C. E., and K. M. Hinkel. 2001. Estimating the variability of active-layer thaw depth in two physiographic regions of northern Alaska. *Geographical Analysis* 33 (2):141–55.

Goodrich, L. E. 1982. The influence of snow cover on the ground thermal regime. *Canadian Geotechnical Journal* 19 (4):421–32.

Grebenets, V. I. 2003. Geocryological–geoecological problems occurring in urbanized territories in Northern Russia and methods for improvement and restoration of foundations. In *Proceedings of the eighth international conference on permafrost*, ed. M. Phillips, S. M. Springman, and L. U. Arenson, 303–7. Zurich, Switzerland: University of Zurich-Irchel.

Grigull, U., and H. Sandner. 1984. *Heat conduction*. Berlin: Springer.

Henry, K., and M. Smith. 2001. A model-based map of ground temperatures for the permafrost regions of Canada. *Permafrost and Periglacial Processes* 12 (4):389–98.

Hersher, R. 2016. Barrow, Alaska, changes its name back to its original "Utqiaġvik." Accessed February 18, 2018. http://www.npr.org/sections/thetwo-way/2016/12/01/503979353/barrow-alaska-changes-its-name-back-to-its-original-utqiagvik.

Hinkel, K. M., J. G. Bockheim, K. M. Petersen, and D. W. Norton. 2003. Impact of snow fence construction on tundra soil temperatures at Barrow, Alaska. In *Proceedings of the Eighth International Conference on Permafrost*, ed. M. Phillips, S. M. Springman, and L. U. Arenson, 401–5. Lisse, The Netherlands: A. A. Balkema.

Hinkel, K. M., W. R. Eisner, J. G. Bockheim, F. E. Nelson, K. M. Peterson, and X. Dai. 2003. Spatial extent, age, and carbon stocks in drained thaw lake basins on the Barrow Peninsula, Alaska. *Arctic, Antarctic, and Alpine Research* 35 (3):291–300.

Hinkel, K. M., and J. K. Hurd, Jr. 2006. Permafrost destabilization and thermokarst following snow fence installation, Barrow, Alaska, U.S.A. *Arctic, Antarctic, and Alpine Research* 38 (4):530–39.

Hinkel, K. M., A. E. Klene, and F. E. Nelson. 2004. The summer climate of an Arctic coastal village. Preliminary observations from the Barrow urban heat-island study. *Polar Geography* 28 (3):197–221.

Hinkel, K. M., and F. E. Nelson. 2003. Spatial and temporal patterns of active layer thickness at Circumpolar Active Layer Monitoring (CALM) sites in Northern Alaska 1995–2000. *Journal of Geophysical Research—Atmospheres* 108 (D2):8168. doi:10.1029/2001JD0000927 2003.

———. 2007. Anthropogenic heat island at Barrow, Alaska during winter: 2001–2005. *Journal of Geophysical Research—Atmospheres* 112 (D6):D06118. doi:10.1029/2006JD007837.

Hinkel, K. M., F. E. Nelson, A. E. Klene, and J. H. Bell. 2003. The winter urban heat island at Barrow, Alaska. *International Journal of Climatology* 23 (15): 1889–1905.

Hinkel, K. M., F. E. Nelson, Y. Shur, J. Brown, and K. R. Everett. 1996. Temporal changes in moisture content of the active layer and near-surface permafrost at Barrow, Alaska: 1962–1994. *Arctic and Alpine Research* 28 (3):300–310.

Hjort, J., O. Karjalainen, J. Aalto, S. Westerman, V. E. Romanovsky, F. E. Nelson, B. Etzelműller, and M. Luoto. 2018. Degrading permafrost puts Arctic infrastructure at risk by mid-century. *Nature Communications* 9:5147. doi: 10.1038/s41467-018-07557-4.

Hollister, R. D., P. J. Webber, R. T. Slider, F. E. Nelson, and C. E. Tweedie. 2008. Soil temperature and thaw response to manipulated air temperature and plant cover at Barrow and Atqasuk, Alaska. In *Proceedings of the Ninth International Conference on Permafrost*, ed. D. L. Kane and K. M. Hinkel, 729–34. Fairbanks: University of Alaska Press.

Hong, E., R. Perkins, and S. Trainor. 2014. Thaw settlement hazard of permafrost related to climate warming in Alaska. *Arctic* 67 (1):93–103.

Hwang, C. T. 1976. Predictions and observations on the behaviour of a warm gas pipeline on permafrost. *Canadian Geotechnical Journal* 13 (4):452–80.

Jumikis, A. R. 1977. *Thermal geotechnics*. New Brunswick, NJ: Rutgers University Press.

Karunaratne, K. C., and C. R. Burn. 2004. Relations between air and surface temperature in discontinuous permafrost terrain near Mayo, Yukon Territory. *Canadian Journal of Earth Sciences* 41 (12):1437–51.

Kersten, M. S. 1949. Laboratory research for the determination of the thermal properties of soils. Technical Report 23, U.S. Army Arctic Construction and Frost Effects Laboratory, Boston, MA.

Klene, A. E., K. M. Hinkel, and F. E. Nelson. 2003. The Barrow Urban Heat Island Study: Soil temperatures and active-layer thickness. In *Proceedings of the Eighth International Conference on Permafrost*, ed. M. Phillips, S. M. Springman, and L. U. Arenson, vol. 1, 555–60. Lisse, The Netherlands: A. A. Balkema.

Klene, A. E., F. E. Nelson, and K. M. Hinkel. 2013. Urban–rural contrasts in summer soil-surface temperature and active-layer thickness, Barrow, Alaska, U.S.A. *Polar Geography* 36 (3):183–201.

Klene, A. E., F. E. Nelson, and N. I. Shiklomanov. 2001. The n-factor as a tool in geocryological mapping: Seasonal thaw in the Kuparuk River Basin, Alaska. *Physical Geography* 22 (6):449–66.

Klene, A. E., F. E. Nelson, N. I. Shiklomanov, and K. M. Hinkel. 2001. The n-factor in natural landscapes: Variability of air and soil-surface temperatures, Kuparuk River Basin, Alaska. *Arctic, Antarctic, and Alpine Research* 33 (2):140–48.

Lachenbruch, A. H. 1957. Three-dimensional heat conduction in permafrost beneath heated buildings. *U.S. Geological Survey Bulletin* 1083A:36.

Lachenbruch, A. H., and B. V. Marshall. 1969. Heat flow in the Arctic. *Arctic* 22:300–311.

———. 1986. Changing climate: Geothermal evidence from permafrost in the Alaskan Arctic. *Science* 234 (4777):689–96.

Lara, M. J., A. D. McGuire, E. S. Euskirchen, C. E. Tweedie, K. M. Hinkel, A. N. Skurikhin, V. E. Romanovsky, G. Grosse, W. R. Bolton, and H. Genet. 2015. Polygonal tundra geomorphological change in response to warming alters future CO_2 and CH_4 flux on the Barrow Peninsula. *Global Change Biology* 21 (4):1634–51. doi:10.1111/gcb.12757.

Lara, M. J., I. Nitze, G. Grosse, and A. D. McGuire. 2018. Tundra landform and vegetation productivity trend maps for the Arctic coastal plain of northern Alaska. *Scientific Data* 5:180058. doi:10.1038/sdata.2018.58.

Lara, M. J., S. Villarreal, D. R. Johnson, R. D. Hollister, P. J. Webber, and C. E. Tweedie. 2012. Estimated change in tundra ecosystem function near Barrow, Alaska, between 1972 and 2010. *Environmental Research Letters* 7 (1):015507 doi:10.1088/18748-9326/7/015507.

Lewellen, R. I. 1972. *Studies on the fluvial environment: Arctic coastal plan province, Northern Alaska*. Palmer, AK: Lewellen Arctic Research.

Liu, L., K. Schaefer, A. Chen, A. Gusmeroli, E. Jafarov, S. Panda, A. Parsekian, T. Schaefer, H. A. Zebker, and T. Zhang. 2015. *Pre-ABoVE: Remotely sensed active layer thickness, Barrow, Alaska, 2006–2011*. Oak Ridge, TN: ORNL DAAC. Accessed May 26, 2018. http://dx.doi.org/10.3334/ORNLDAAC/1266.

Lord, N. W., J. P. Pandolfo, and M. A. Atwater. 1972. Simulations of meteorological variations over Arctic coastal tundra under various physical interface conditions. *Arctic and Alpine Research* 4 (3):189–210.

Lunardini, V. J. 1981. *Heat transfer in cold climates*. New York: Van Nostrand Reinhold.

Lunardini, V. J., and R. Varotta. 1981. Approximate solution to Neumann problem for soil systems. *Journal of Energy Resource Technology* 103 (1):76–81.

Mazhitova, G., G. Malkova, O. Chestnykh, and D. Zamolodchikov. 2004. Active-layer spatial and temporal variability at European Russian Circumpolar-Active Layer-Monitoring (CALM) sites. *Permafrost and Periglacial Processes* 15 (2):123–29.

McGaw, R. W., S. I. Outcalt, and E. Ng. 1978. Thermal properties and regime of wet tundra soils at Barrow, Alaska. In *Proceedings of the Third International Conference on Permafrost*, 47–53. Ottawa, ON, Canada: National Research Council of Canada.

Muller, S. V., D. A. Walker, F. E. Nelson, N. A. Auerbach, J. Bockheim, S. Guyer, and D. Sherba. 1998. Accuracy assessment of a land-cover map of the Kuparuk River basin, Alaska: Considerations for remote regions. *Photogrammetric Engineering and Remote Sensing* 68:619–28.

Muller, S. W. 1943. Permafrost or perennially frozen ground and related engineering problems. Strategic Engineering Study No. 62 Special Report, U.S. Army, Intelligence Branch, Office of the Chief of Engineers.

———. 2008. *Frozen in time: Permafrost and engineering problems*, ed. H. M. French and F. E. Nelson. Reston, VA: American Society of Civil Engineers Technical Committee on Cold Regions Engineering.

Nakano, Y., and J. Brown. 1972. Mathematical modeling and validation of the thermal regimes in tundra soils, Barrow, Alaska. *Arctic and Alpine Research* 4 (1):19–38.

National Centers for Environmental Information. 2018. Climate data online, Barrow Wiley Post–Will Rogers Airport, 1981–2010 normals. Accessed February 18, 2018. https://www.ncdc.noaa.gov/cdo-web/datatools/normals.

Nelson, F. E. 1986. Permafrost distribution in central Canada: Applications of a climate-based predictive model. *Annals of the Association of American Geographers* 76 (4):550–69.

Nelson, F. E., O. A. Anisimov, and N. I. Shiklomanov. 2001. Subsidence risk from thawing permafrost. *Nature* 410 (6831):889–90.

———. 2002. Climate change and hazard zonation in the circum-Arctic permafrost regions. *Natural Hazards* 26 (3):203–25.

Nelson, F. E., K. M. Hinkel, N. I. Shiklomanov, G. R. Mueller, L. L. Miller, and D. A. Walker. 1998. Active-layer thickness in north-central Alaska: Systematic sampling, scale, and spatial autocorrelation. *Journal of Geophysical Research: Atmospheres* 103 (D22):28963–73.

Nelson, F. E., N. I. Shiklomanov, and G. R. Mueller. 1999. Variability of active-layer thickness at multiple spatial scales, north-central Alaska, U.S.A. *Arctic, Antarctic, and Alpine Research* 31:158–65.

Nelson, F. E., N. I. Shiklomanov, G. R. Mueller, K. M. Hinkel, D. A. Walker, and J. G. Bockheim. 1997. Estimating active-layer thickness over a large region: Kuparuk River basin, Alaska, U.S.A. *Arctic and Alpine Research* 29 (4):367–78.

Nelson, F. E., N. I. Shiklomanov, D. A. Streletskiy, V. E. Romanovsky, K. Yoshikawa, K. M. Hinkel, and J. Brown. 2008. A permafrost observatory at Barrow, Alaska: Long-term observations of active-layer thickness and permafrost temperature. In *Proceedings of the Ninth International Conference on Permafrost*, ed. D. L. Kane and K. M. Hinkel, 1267–72. Fairbanks: University of Alaska Press.

NEON. 2018. Barrow Environmental Observatory—BARR. Accessed February 18, 2018. http://www.neonscience.org/field-sites/field-sites-map/barrow-environmental-observatory.

Next Generation Ecosystem Experiments. 2018. NGEE Arctic. Next Generation Ecosystem Experiments. Accessed February 18, 2018. https://ngee-arctic.ornl.gov/.

Norton, D. W., ed. 2001. *Fifty more years below zero: Tributes and meditations for the Naval Arctic Research Laboratory's first half century in Barrow, Alaska*. Calgary, AB, Canada: The Arctic Institute of North America.

Nyland, K. E., A. E. Klene, J. Brown, N. I. Shiklomanov, F. E. Nelson, D. E. Streletskiy, and K. Yoshikawa. 2017. Traditional Iñupiat ice cellars (*Siġ-uaq*) in Barrow, Alaska: Characteristics, temperature monitoring, and distribution. *Geographical Review* 107 (1):143–58. doi:10.1111/j19310846.2016.12204.x.

Olefeldt, D., S. Goswami, G. Grosse, D. Hayes, G. Hugelius, P. Kuhry, A. D. McGuire, V. E. Romanovsky, A. B. K. Sannel, E. A. G. Schuur, and M. R. Turetsky. 2016. Circumpolar distribution and carbon storage of thermokarst landscapes. *Nature Communications* 7:13043. doi:10.1038/ncomms13043.

Oliver, S. G. 2017. One year later, Utqiaġvik keeps its name. *The Arctic Sounder*, October 20. Accessed September 14, 2018. http://www.thearcticsounder.com/article/1742one_year_later_utqiagvik_keeps_its_name 14, 2018.

Outcalt, S. I. 1972. The development and application of a simple digital surface climate simulation. *Journal of Applied Meteorology* 11 (4):629–36.

Outcalt, S. I., and C. Goodwin. 1980. A climatological model of surface modification effects on the thermal regime of the active layer at Barrow, Alaska. In *ASME Petroleum Division Energy Technology Conference & Exhibition New Orleans, Louisiana*, 1–9. New York: American Society of Mechanical Engineers.

Outcalt, S. I., D. H. Gray, and W. S. Benninghoff. 1989. Soil temperature and electric potential during diurnal and seasonal freeze-thaw. *Cold Regions Science and Technology* 16 (1):37–43.

Paynter, H. M. 1999. A retrospective on early analysis and simulation of freeze and thaw dynamics. In *Proceedings of the 10th International Conference on Cold Regions Engineering*, ed. J. E. Zufelt, 160–72. Lincoln, NH: American Society of Civil Engineering.

Péwé, T. L. 1966. *Permafrost and its effect on life in the North*. Corvallis: Oregon State University Press.

Polar Geospatial Center. 2018. Arctic DEM. Accessed June 17, 2018. https://www.pgc.umn.edu/data/arcticdem/.

Ray, P. H., J. Murdoch, C. V. Riley, A. Gray, W. H. Dall, and C. A. Schott. 1885. Report of the *International Polar Expedition to Point Barrow, Alaska in response to the resolution of the House of Representatives of December 11, 1884*. Washington, DC: U.S. Government Printing Office.

Raynolds, M. K., D. A. Walker, K. J. Ambrosius, J. Brown, K. E. Everett, M. Kanevskiy, G. P. Kofinas, V. E. Romanovsky, Y. Shur, and P. J. Webber. 2014. Cumulative geoecological effects of 62 years of infrastructure and climate change in ice-rich permafrost landscapes, Prudhoe Bay oilfield, Alaska. *Global Change Biology* 20 (4):1211–24.

Romanovsky, V. E. 2011. High-resolution permafrost modeling and planning implications for Greenland and Alaska. *Witness the Arctic: Spring* 2011 (2). https://www.arcus.org/witness-thearctic/2011/2/article/1651

Schaefer, K., L. Liu, A. Parsekian, E. Jafarov, A. Chen, T. Zhang, A. Gusmeroli, S. Panda, H. A. Zebker, and T. Schaefer. 2015. Remotely sensed active layer thickness (ReSALT) at Barrow, Alaska using interferometric synthetic aperture radar. *Remote Sensing* 7 (4):3735–59. doi:10.3390/rs70403735.

Sellmann, P. V., J. Brown, R. I. Lewellen, H. L. McKim, and C. J. Merry. 1975. The classification and geomorphic implications of thaw Lakes on the Arctic coastal plain, Research Report 344, U.S. Army Cold Regions Research and Engineering Laboratory, Hanover, NH.

Shiklomanov, N. I., and F. E. Nelson. 1999. Analytic representation of the active layer thickness field, Kuparuk River basin, Alaska. *Ecological Modelling* 123 (2–3):105–25.

Shiklomanov, N. I., F. E. Nelson, D. A. Streletskiy, K. M. Hinkel, and J. Brown. 2008. The Circumpolar Active Layer Monitoring (CALM) program: Data collection, management, and dissemination strategies. In *Proceedings of the Ninth International Conference on Permafrost*, ed. D. L. Kane and K. M. Hinkel, 1647–52. Fairbanks: University of Alaska Press.

Shiklomanov, N. I., D. A. Streletskiy, V. I. Grebenets, and L. Suter. 2017. Conquering the permafrost: Urban infrastructure development in Norilsk, Russia. *Polar Geography* 40 (4):273–90.

Shiklomanov, N. I., D. A. Streletskiy, J. D. Little, and F. E. Nelson. 2013. Isotropic thaw subsidence in undisturbed permafrost landscapes. *Geophysical Research Letters* 40:1–6. doi:10.1002/2013GL058295.

Shiklomanov, N. I., D. A. Streletskiy, F. E. Nelson, R. D. Hollister, V. E. Romanovsky, C. E. Tweedie, J. G. Bockheim, and J. Brown. 2010. Decadal variations of active-layer thickness in moisture-controlled landscapes, Barrow Alaska. *Journal of Geophysical Research—Biogeochemical Cycles* 115:G00I04. doi:10.1029/2009JG001248

Shiklomanov, N. I., D. A. Streletskiy, T. B. Swales, and V. A. Kokorev. 2017. Climate change and stability of infrastructure in Russian permafrost regions: Prognostic assessment based on GCM climate projections. *Geographical Review* 107 (1):125–42. doi:10.1111/gere.12214.

Shur, Y. L., and V. B. Slavin-Borovskiy. 1993. *N-factor maps of Russian permafrost region*. In *Proceedings of the Sixth International Conference on Permafrost*, vol. 1, 564–68. Wushan: South China University of Technology Press.

Smith, G. M., and R. E. Rager. 2002. Protective layer design in landfill covers based on frost penetration. *Journal of Geotechnical and Geoenvironmental Engineering* 128 (9):794–99.

Sonnenfeld, J. 1960. Changes in an Eskimo hunting technology: An introduction to implement geography. *Annals of the Association of American Geographers* 50 (2):172–86.

Stone, R. S., E. G. Dutton, J. Harris, and D. Longenecker. 2002. Earlier spring snowmelt in Northern Alaska as an indicator of climate change.

Journal of Geophysical Research 107 (D10):ACL 10-1–ACL 10-13. doi:10.1029/2000JD000286.
Stow, D. A., A. Hope, D. McGuire, D. Verbyla, J. Gamon, K. F. Huemmrich, S. Houston, et al. 2004. Remote sensing of vegetation and land-cover change in Arctic tundra ecosystems. *Remote Sensing of Environment* 89 (3):281–308.
Streletskiy, D. A., N. I. Shiklomanov, J. D. Little, F. E. Nelson, J. Brown, K. E. Nyland, and A. E. Klene. 2017. Thaw subsidence in undisturbed tundra landscapes, Barrow, Alaska, 1962–2015. *Permafrost and Periglacial Processes* 28 (3):566–72. doi:10.1002/ppp.1918.
Streletskiy, D. A., N. I. Shiklomanov, and F. E. Nelson. 2012. Permafrost, infrastructure, and climate change: A GIS-based landscape approach to geotechnical modeling. *Arctic, Antarctic, and Alpine Research* 44 (3):368–80.
Tedrow, J. C. F., and J. E. Cantlon. 1958. Concepts of soil formation and classification in Arctic regions. *Arctic* 11 (3):166–79.
U.S. Arctic Research Commission Permafrost Task Force. 2003. *Climate change, permafrost, and impacts on civil infrastructure*. Arlington, VA: U.S. Arctic Research Commission.
U.S. Bureau of Land Management. 1998. *NPR-A earth cover classification*. Anchorage, AK: U.S. Bureau of Land Management. Accessed February 18, 2018. http://agdc.usgs.gov/data/usgs/erosafo/ak_lcc/metadata/npra_blm.html.
U.S. Census Bureau. 2018. Community facts, Barrow city, Alaska. 2016 population estimate. Accessed February 18, 2018. https://factfinder.census.gov/faces/nav/jsf/pages/community_facts.xhtml.
U.S. Geological Survey. 1955. *Barrow (B-4) Quadrangle. Scale 1:63,360*. Washington, DC: U.S. Geological Survey.
Utqiaġvik. 2018. About Utqiaġvik. Accessed February 18, 2018. http://www.utqiagvik.us/index.php/about-barrow.
van Everdingen, R. O., ed. 1994. *Multi-language glossary of permafrost and related ground ice terms*. Calgary, AB, Canada: International Permafrost Association Terminology Working Group, University of Calgary Printing Services.
Vieira, G., J. Bockheim, M. Guglielmin, M. Balks, A. A. Abramov, J. Boelhouwers, N. Cannone, et al. 2010. Thermal state of permafrost and active-layer monitoring in the Antarctic: Advances during the International Polar Year 2007–2009. *Permafrost and Periglacial Processes* 21 (2):182–97. doi:10.1002/ppp.685.
Villarreal, S., R. D. Hollister, D. R. Johnson, M. J. Lara, P. J. Webber, and C. E. Tweedie. 2012. Tundra vegetation change near Barrow, Alaska (1972–2010). *Environmental Research Letters* 7:015508. doi:10.1088/1748-9326/7/1/015508.
Waelbroeck, C. 1993. Climate-soil processes in the presence of permafrost: A systems modeling approach. *Ecological Modelling* 69 (3–4):185–225.
Walker, D. A., and K. R. Everett. 1987. Road dust and its environmental impact on Alaskan taiga and tundra. *Arctic and Alpine Research* 19 (4):479–89.
Walker, D. A., W. A. Gould, H. A. Maier, and M. K. Raynolds. 2002. The circumpolar Arctic vegetation map: AVHRR-derived base maps, environmental controls, and integrated mapping procedures. *International Journal of Remote Sensing* 23 (21):4551–70.
Walsh, J. E. 1977. Measurements of the temperature, wind, and moisture distribution across the northern coast of Alaska. *Arctic and Alpine Research* 9 (2):175–82.
Webber, P. J., P. C. Miller, F. S. Chapin, III, and B. H. McCown. 1980. The vegetation: Pattern and succession. In *An Arctic ecosystem: The coastal tundra at Barrow, Alaska*, ed. J. Brown, P. C. Miller, L. L. Tieszen, and F. L. Bunnell, 186–218. Stroudsburg, PA: Dowden, Hutchinson and Ross.
Yershov, E. D. 1998. *General geocryology*. New York: Cambridge University Press.
Yi, S., K. Wischnewski, M. Langer, S. Muster, and J. Boike. 2014. Freeze/thaw processes in complex permafrost landscapes of Northern Siberia simulated using the TEM ecosystem model: Impact of thermokarst ponds and lakes. *Geoscientific Model Development* 7 (4):1671–89. doi:10.5194/gmd-7-1671-2014.
Yoshikawa, K., V. Romanovsky, N. Duxbury, J. Brown, and A. Tsapin. 2004. The use of geophysical methods to discriminate between brine layers and freshwater taliks in permafrost regions. *Journal of Glaciology and Geocryology* 26:301–9.
Zarling, J. P., W. A. Braley, and C. Pelz. 1989. The modified Berggren method: A review. In *Cold regions engineering: Proceedings of the 5th international conference*, ed. R. L. Michalowski, 262–73. Reston, VA: American Society of Civil Engineering.

ANNA E. KLENE is Professor in the Department of Geography at University of Montana, Missoula, MT 59812. E-mail: anna.klene@umontana.edu. Her research interests include permafrost, climatology, and remote sensing.

FREDERICK E. NELSON is Adjunct Professor in the Department of Geography, Environment, and Spatial Sciences at Michigan State University, East Lansing, MI 48824; Research Associate in the Department of Earth, Environmental, and Geographical Sciences at Northern Michigan University, Marquette, MI 49855; and Adjunct Professor and Research Fellow in the Department of Geography and American Geographical Society Library at the University of Wisconsin–Milwaukee, Milwaukee, WI 53201. E-mail: fnelson@msu.edu. His research interests include permafrost, periglacial geomorphology, and the history of Arctic science.